Three-Dimensional Modeling and Analysis of Mechanized Excavation for Tunnel Boring Machines

Danial S Mohammadzadeh, Nader Karballaeezadeh, Amirhossein Sanaei Zahed, Amir Mosavi and Imre Felde

April 28, 2020

Three-Dimensional Modeling and Analysis of Mechanized Excavation for Tunnel Boring Machines

Danial Mohammadzadeh S [1,2,3,4], Nader Karballaeezadeh [4,5], Amirhossein Sanaei Zahed [4,6], Amir Mosavi [7], Felde Imre [8]

[1] Department of Civil Engineering, Ferdowsi University of Mashhad, Mashhad, University street. 1, P.O. BOX 9177948974, Iran.

danial.mohammadzadehshadmehri@mail.um.ac.ir

[2] Department of Civil Engineering, Mashhad Branch, Islamic Azad University, Mashhad, University street. 1, P.O. BOX 9187147578, Iran.

[3] Department of Civil Engineering, Faculty of Montazeri, Khorasan Razavi Branch, Technical and Vocational University (TVU), Mashhad, University street. 1, P.O. BOX 9176994594, Iran.

[4] Department of Elite Relations with Industries, Khorasan Construction Engineering Organization, Mashhad, University street. 1, P.O. BOX 9185816744, Iran.

N.karballaeezadeh@shahroodut.ac.ir

[5] Faculty of Civil Engineering, Shahrood University of Technology, Shahrood, University street. 1, P.O. BOX 3619995161, Iran.

[6] Toos Institite of Higher Education, Khorasan Razavi, Mashhad, University street. 1, P.O. BOX 9188911111, Iran.

Ah.sanaei@toos.ac.ir

[7] Institute of Automation, Kalman Kando Faculty of Electrical Engineering, Obuda University, Becsi street 96/b, Budapest 1034, Hungary.

amir.mosavi@kvk.uni-obuda.hu

[8] John von Neumann Faculty of Informatics, Obuda University, Becsi street 96/b, 1034 Budapest, Hungary.

felde@uni-obuda.hu

Urban train infrastructures are of utmost importance for reliable mobility in the smart cities of the future. This paper is about Three-dimensional Modeling of Mechanized Drilling Passes. Drilling in an urban is always a risky and complex experience. One of the most *important issues during the construction of subway tunnels is the investigation of the impact of drilling steps on the ground subsidence and its containment. For this purpose, different types of mechanized drilling methods are often used, resulting in a considerable reduction in the displacements caused by tunnel drilling. In this study, part of the route of an urban train tunnel that passes under a non-planar intersection is examined. The shear capacity of slab pile, slab piles was calculated using the relevant equations and then modeling of soil mass was performed using the PLAXIS 3D software finite element program. The proposed depth of the tunnel construction by the consulting company is 18 meters. Due to drilling problems, the presence of overpass piles near the tunnel and experience of 14 meters depth has been used as an alternative. Analyzes for both 14 and 18 m depths showed that the displacements at both depths were approximately the same. So, the impact of the tunnel on the pile capacity of the bridge piles at a depth of 18 m is greater than the depth of 14 m. Thus, the depth suggested by the authors is 14 meters, which is more suitable than the initial depth of 18 meters.*

Keywords: Tunnel; mechanized drilling; modeling; plaxis software; optimization; urban train lines; computational mechanics; simulation; smart cities.

1 Introduction

Urbanization and urban development have necessitated the need for effective public transportation systems [1-3]. The urban train network is one of the most important transportation systems in cities [4-7]. Because of land restriction and increasing surface congestion, the underground train network is more preferable to build the underground one [8]. Drilling in urban areas is complex and risky. The effect of drilling operations on the ground surface settlement is one of the most critical matters during the construction of metro tunnels. To reduce this problem, drilling mechanization methods have been developed in recent decades.

Urban trains line 2 city of has a length of approximately 14 kilometers, comprising 13 stations. Part of the Shiraz Metro Line 2 route starts north of Azadi Square and connects to the Shiraz Metro Line 1 in Imam Hossein Square. It then connects to the airport on Fatemi Avenue and, after crossing the Amir Kabir Pass, to the jail and Adelabad intersection and the Mianrood Sports Complex (Figure 1). According to geotechnical studies, tunnel excavation from Champions Station to Azadi Station was designed by EPB and TBM machines with a diameter of 6.88 m in two twin tunnels. Tunnel boring machine (TBM) drilling in the soil is always associated with sedimentation, so controlling possible displacements and meetings for the construction of an underground structure in urban environments, especially in areas where important structures are at ground level, is one of the critical parameters in project development, especially in the project that both TBMs must pass under the span of this bridge.

The Bridge Road Belt is a type of friction on the bridge road (Mianrood Bridge) and should be considered in the tunnel path design under this bridge "to reduce displacements at ground level and slab piles as well as replace reduce impacts on the bearing capacity of the pile". According to the tunnel plan and profile designed by the consultant, the height of the tunnel under the Mianrood Bridge is 18.1 m and the tunnel wall to the side piles of the bridge is approximately 5 m and the tunnel distance to the middle piles of the bridge is approximately 3 m. According to Geotechnical studies, BH 15 borehole has been excavated in the area of the bridge, the area of which is 29 m deep to Lean Clay, at a depth of 29 m to 30 m, a silty sand layer. The groundwater level in this borehole is about 4.75 meters.

In this study, 3D modeling of TBM crossing conditions under bridge foundations was performed at two depths of 14 m (research authors' recommendation) and 18 m (consulting firm recommendation).

In this study, 3D modeling of TBM crossing conditions under bridge foundations was carried out at two depths of 14 m and 18 m.

Figure 1
Location of urban train line 2 city of Shiraz

2 Tunnel Summary Analysis of Drilling TBM and Pile and Tunnel base interaction

The effective factors in the tunneling sessions are divided into three zones as shown in Fig. (2).

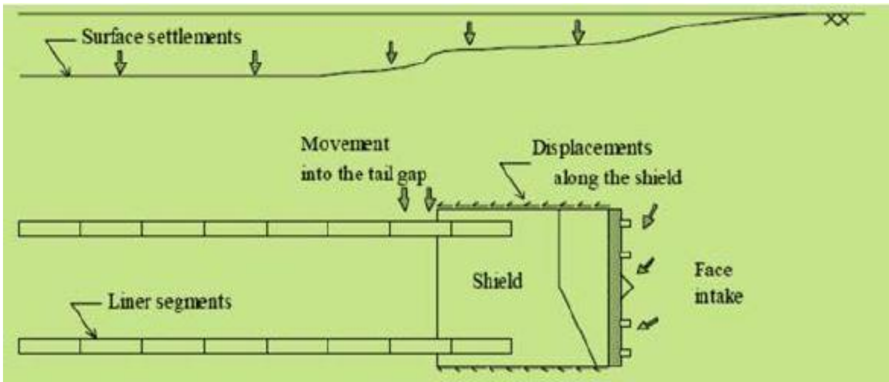

Figure 2
Various settlement Areas Created in Tunneling by Sheild Method [9]

Zone 1

The settlement caused by displacements created on the tunnel front. If the tunnel front pressure is inadequate or the operator does not operate correctly and the volume of soil exited from the work site exceeds the desired soil volume, displacements on the front to ground level may continue.

Occasionally, low pressure of the work surface will overcome the water and soil pressure and the front falls to the shield. Thus, after the shield passes through the area, the soil will be stressed and displaced and will settle again (Figure 3). Of course, high pressure, on the work surface will also lead to a severe depreciation of the cutting tools and device depreciation.

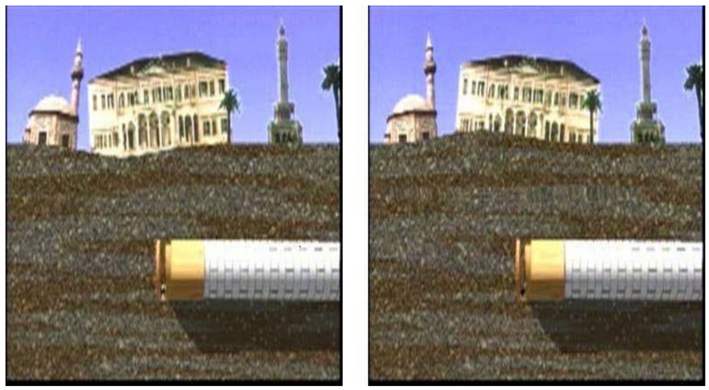

Figure 3
Effects of up and down pressure on the front

Zone 2

This area is within the shield length range (Figure 2). Usually, for easier movement of the shield, the drilling diameter is 1 or 3 cm larger than the outer diameter of the shield ends. They also form a spindle metal cylinder that shields the front and rear friction. For this reason, this area of several meters around the shield and the movement of the shield and its impact on ground displacements can cause the settlement in this area. Bentonite slurry injected around the shield during drilling can be used to prevent this subsidence and to prevent soil shield friction [10].

Zone 3

Due to the difference between the outer diameter of the concrete rings (6.6 m in this project) and the drilling diameter (about 6.88 m), there is a distance between the concrete rings and the soil which is determined by the grout slurry with the specified pressure according to the pressure. Hydrostatic water and soil fill during drilling and shield movement (Figure 2).

The summit in this region depends on the geological, resistive and grouting properties of the summit, with sums summing up with summit zones 1 and 2 of the whole summit resulting from tunneling operations using the earth balance shield method [10].

3 Interaction Analysis of Tunnel and Pile

In general, the interaction between piles and tunnels has been studied in several studies. The basis of these studies is the depth of the tunnel, the depth of the piles, the horizontal distance of the tunnel to the pile and the effect of tunnel drilling interaction on pile displacement [11]. Figure 4 illustrates the different types of the tunnel and pile placement.

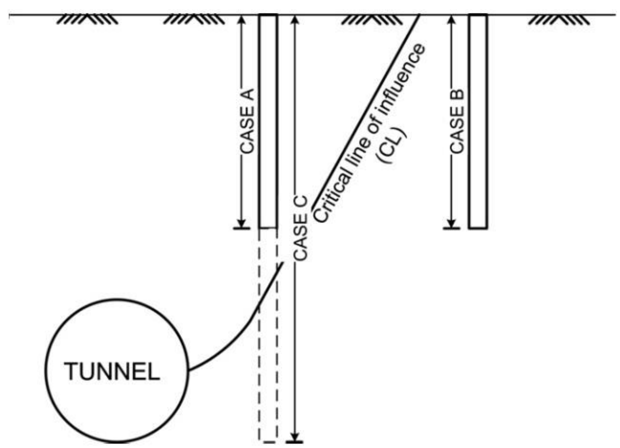

Figure 4
Tunnel and Pile modes and tunnel impact area [3]

In modes A and B in the figure (4) the tunnel is below the tip of the pile. In case A, the tunnel excavation and the displacement caused by the friction of the pile wall as well as the bearing capacity of the pile tip can affect the pile failure and even in some cases cause pile failure. In the case of B, the radius of the impact of the tunnel displacement has less effect on the pile, and the pile is not in the critical area of the tunnel effect. Thus, in these two cases, the horizontal distance of the tunnel from this pile is less effective on the piles. In the C state of Fig. (4) the tunnel can affect the bearing capacity of the friction wall of the pile and also the bearing capacity of the pile tip.

The closer the horizontal distance of the tunnel to the pile, the greater the impact, and the closer the tunnel to the pile tip, the greater the impact on the bearing capacity of the pile tip and the greater the bending moment on the pile. In most case C, the tunnel should have a horizontal distance from the pile, and the height of the tunnel should be chosen so that it has the least impact on the bearing of the capacity of the pile and also has the least siting and displacement on the pile head and ground [11].

Figure 5 shows a schematic of the effects of the tunnel impact zone and the ratio of pile head displacement to ground displacement due to tunnel excavation and subsidence phenomena. In this figure, if the piles are in area A and above the tunnel impact surface, it is possible to move the pile head further than the ground surface displacement above the tunnel (R>1) And in area B, the displacement is equal (R=1) And in area C it has less pile head displacement than the ground level displacement above the tunnel (R<1) [12].

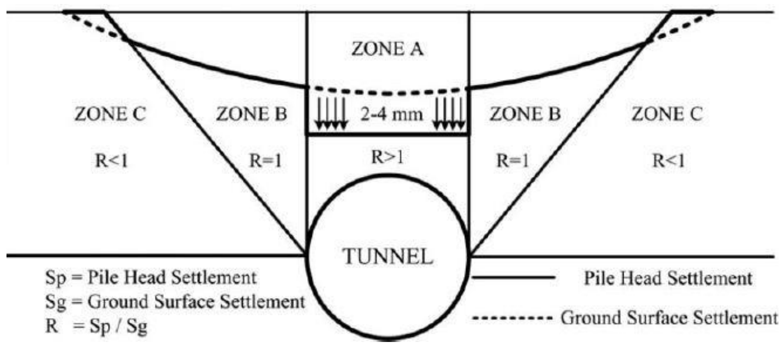

Figure 5
The Tunnel impact areas on the ground as well as the piles [12]

Effect of Tunnels zones on earth settlement and piles settlement

4 The geometry of Belt Road Bridge (Mianrood Bridge) and Calculation of Loads on Piles and Slabs

Mianrood Bridge is located on the Ring Road around Shiraz. Figure (6) shows a view of the span of the Mianrood Bridge. The bridge piles are frictional, and the schematic of the pile arrangement on the slabs and the geometrical properties of the bridge are shown in Fig. 7.

Figure 6
View of Mianrood Bridge and its crater on the Belt Road

The base slabs of the middle of the bridge have dimensions of 6.8 * 16.4 m and are spun on 8 piles 1.2 m in diameter and 25 m in length. The side slabs are 6.8 * 17.43 m on 10 piles with a diameter of 1.2 m and a length of 27 m.

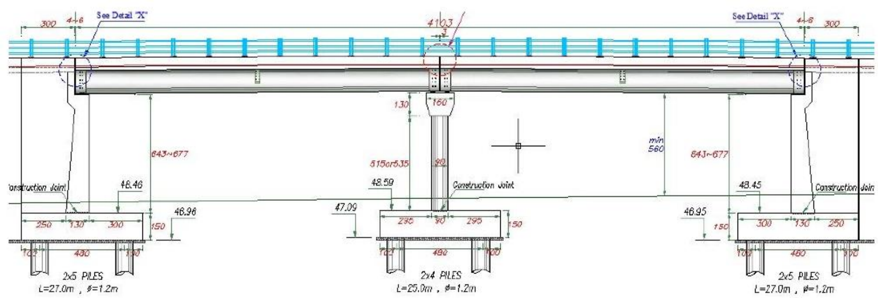

Figure 7
Geometry of Bridge Road Belt (Mianrood Bridge)

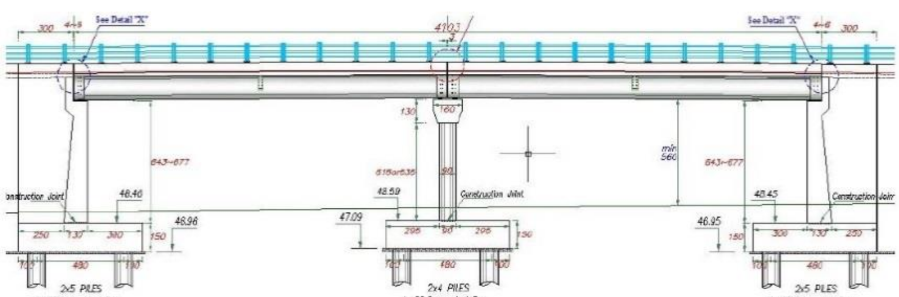

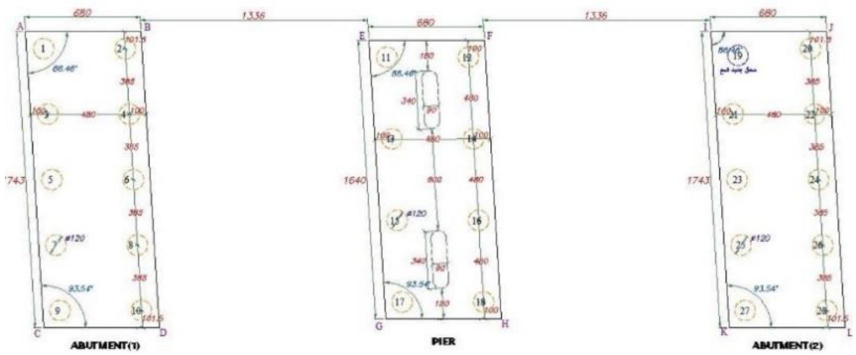

Figure 8

The geometry of Bridge Road Belt (Mianrood Bridge)

5 Calculate Load on Floor Slabs

Calculation of load on floor slabs for 3D modeling and tunnel front pressure calculation. In the reverse method, considering the diameter of each pile as well as its length and Geotechnical characteristics of the local soil, the ultimate and the permissible bearing capacity of each pile can be estimated, and with this bearing capacity, a wide computational load on each slab can be obtained.

The load capacity of friction piles is obtained from the sum of the final load capacity of the pile wall and the cap of the pile. Using the permissible load, we can calculate the maximum permissible load on the floor slabs of the bridge stands [13].

5.1 Ultimate Bearing Capacity of Pile Cap

Generally, the ultimate bearing capacity of the pile cap is calculated according to (1) [13]:

$$Q_{up} = A_p(N_c^* C_{ub} + 50 N_q^* \tan \varphi) \tag{1}$$

Where Q_{up} is the ultimate bearing capacity of pile cap (Kg), A_p is the base area of pile cap (for pile bridges is 1.2 m in diameter), C_{ub} is the undrained shear strength of soil in the pile cap which according to Geotechnical studies of this area is 75 Kpa. N^*_q and N^*_c Bearing capacity Factors that depend on the friction angle of the soil space and can change you using the internal friction angle. Consider the figure (9) and the angle of internal friction of the site which is approximately 26 degrees.

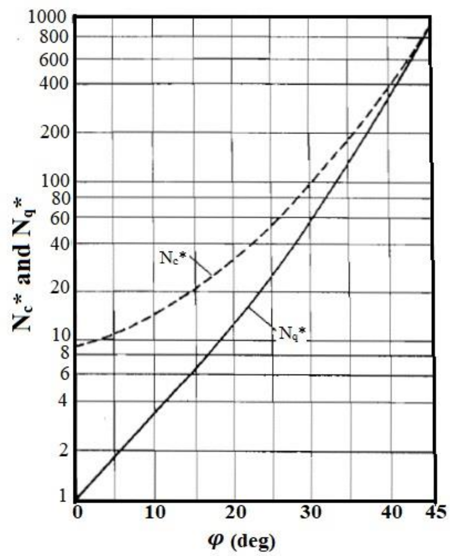

Figure 9
Most variations of $N_c^*$and N_q^*values with internal friction angle [14]

The bearing capacity of the pile cap in this study is equal to:

Q_{up}=1.13×(60×75 + 50×25 tan26) =5774 KN

5.2 Ultimate Bearing Capacity of Pile Wall

To calculate the ultimate bearing capacity of the pile wall in the undrained state, the method was used. This method assumes that the loading behavior of piles in low permeable clays is not similar to piles in drained soils. The ultimate bearing capacity of pile wall in the undrained state is obtained from the relation (2) [13]:

$$Q_{us} = A_s \alpha C_u \quad (2)$$

Where Q_{us} is the ultimate bearing capacity of the wall pile (Kg), A_s is the pile wall area(πDL) in m^2, C_{ub} is the undrained shear strength of soil in pile wall which according to Geotechnical studies of this area is equal to 50 kPa.

Coefficient α: Experimental factor decreased the adhesion of the shaft wall soil to less than one unit. The decrease in shaft wall adhesion is attributable to the softening of the shaft wall in construction operations compared to the undrained shear strength of the soil. According to Fig. 10, the value of this coefficient for the ultimate bearing capacity is considered to be 0.6.

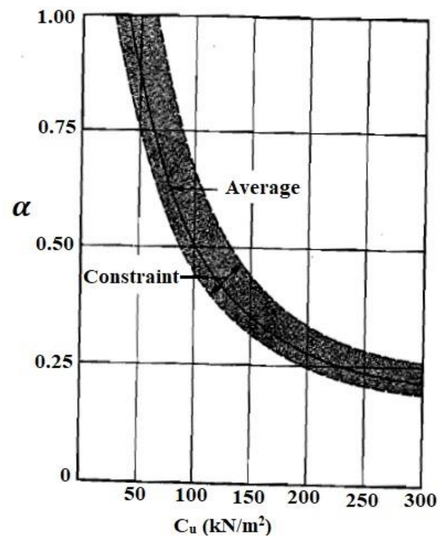

Figure 10
The graph between the value of C_U(KN/m^2) and the coefficient α [14]

Due to the geometry of the bridge road and the designed piles, the middle slab piles are 25 m long and the side slab piles are 27 mm long.

$$Q_{us(25m)} = 25*1.2*3.14*0.6*75 = 4239KN$$

$$Q_{us(27m)} = 27*1.2*3.14*0.6*75 = 4578KN$$

Now, we can Calculate the ultimate bearing capacity of the pile. we can calculate (3) the amount of load allowed per pile.

$$Q_w = \frac{Q_{up} + Q_{us}}{F.S} \tag{3}$$

Where Q_w permits the load allowed on each pile (Kg), Factor of safety (F.S) for each pile with a number between 2.5 and 4 considered 4 in this study. According to the above, the amount of load capacity of the pile is allowed:

$Q_w = (5774 + 4239)/4 = 2503KN$ The load capacity of piles in the middle slab section of the bridge

$Q_w = (5774 + 4578)/4 = 2588KN$ Bearing capacity of piles on slab side bridge

The number of piles in the middle slab is 8 and in the side slab is 10. Also, the middle slab area is 111 m^2 and the side slab area is 129 m^2. Therefore, the load on each slab is equal to the load capacity of each pile and the number of piles:

q = (8*2503)/111= 180 KN/m^2 Middle Slab

q = (10*2588)/129= 200 KN/m^2 Slabs aside

6. 3D Tunnel Modeling

In this section, the optimization of tunnel overburden to reduce TBM system depreciation and reduce TBM drilling pressures under the 18 and 14 meters overpass bridge is investigated by Plaxis3D software. The main reason for lowering the tunnels to a depth of 18 meters is the lesser impact of tunnel drilling on the Mianrod Bridge. Figure (11) shows the geometry of the modeling of the tunnels and the Mianrod Bridge in two overpasses of 14 and 18 m.

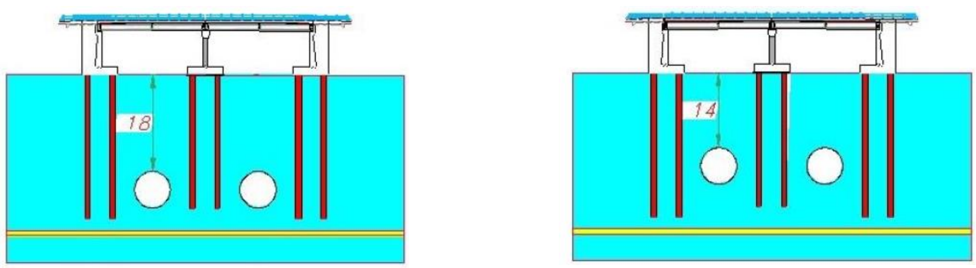

Figure 11
Modeling geometry of tunnels and bridge of Miranrood in two elevations of 14 and 18 meters.

Considering the tunneling steps by EPB method and the capabilities of Plaxis 3D ver 1.2 software in simulating the drilling process (applying working pressure chest, considering the amount of shrinkage, applying injection pressure, drilling and segmentation steps), to calculate the setting parameters from this.

The program is based on the finite element relationships used in the two-dimensional program that, also to the two-dimensional model, is capable of simulating three-dimensional behavior of underground structures in terrestrial environments. Materials are constructed by user-created areas in the model. Each member responds to forces or boundary constraints according to the stress-strain law, either linear or nonlinear. The speed of software computation depends on the number of model areas and the speed of the computer used. The modeling steps are as follows:

Geometry: Due to the overburden and the distance of the tunnels at the cross section 60 m long and 35 m deep are considered for all models. The dimensions are chosen so that unrealistic boundary conditions do not affect the model. Two depths of 14 and 18 meters are provided for the tunnels.

Boundary conditions: After defining two-dimensional and three-dimensional geometry, it comes to the boundary conditions, which are the detailed conditions at the bottom of the model as well as the roller conditions for the sides. According to the calculations made in Section 5, the average slab load is 180 KN / m^2 and the side slab is 200 KN / m^2.

Geotechnical Properties of Aggregates: Material properties include the soil layers of the tunnels as well as the shields and segments according to Tables (1) and (2).

Table 1

Geotechnical properties of soil layers

ID	Type	g_unsat	g_sat	Nu	E_ref	c_ref	φ
		KN/m^3	KN/m^3		KN/m^2	KN/m^2	degree
BH 15-1 (clay)	Drained	15	17	0.28	2.10e04	15	25
BH 15-2 (sand)	Drained	17	20	0.28	1.3ee04	1	31

Table 2

Shield and Segment Specifications

ID	Type	EA	EI	nu
		KN/m	KN.m^2/m	
Plate	Elastic	8200000	83800	0
Segment	Elastic	10570000	107900	0.15

Triangular elements are used to mesh. The model is first trimmed in two-dimensional mode and then expanded to the third dimension. Figure 12 shows the whole model and its three-dimensional mesh.

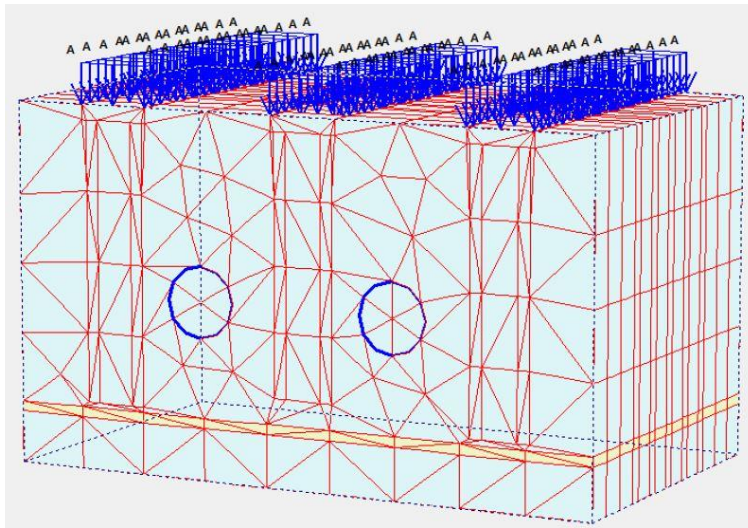

Figure 11
The three-dimensional model of tunnels crossing under the bridge of Mianrood

Preliminary Conditions: Upon completion of the previous steps, generally the initial conditions include the effective stress based on the soil lateral pressure coefficient and the water pressure that the water level is considered by the geological maps in the model.

Computational Phases: At this stage, the actual drilling conditions are attempted to be simulated. Overall, there are three steps to simulating drilling cycles in EPB modeling.

First, it is the shield and a chamber section of the machine that performs the drilling and pressure on the chest. Since the shield length is 9 meters, shield drilling is done in three steps of 3 meters. In this section, shield parameters are considered for the lining. For modeling piles, the lengths of the advances are also proportional to the intervals of the piles. Vacuum injection is modeled behind the segments. In general, there should be a relative balance between the working pressure and injection pressure. The injection pressure is 50 kPa higher than the working pressure. It should be noted that at this stage there is no linearity. At the bottom (after injection of slurry into the vacuum between the segment and the soil around the tunnel) the segments are intended for the lining. Fig. 12 shows a complete drilling cycle with applied front-side work pressure and grout injection pressure and tunnel lining system. According to the analytical equations, the working pressure values of 140 and 170 kPa in the 14 and 18 meters overburden are considered in the tunnel crest.

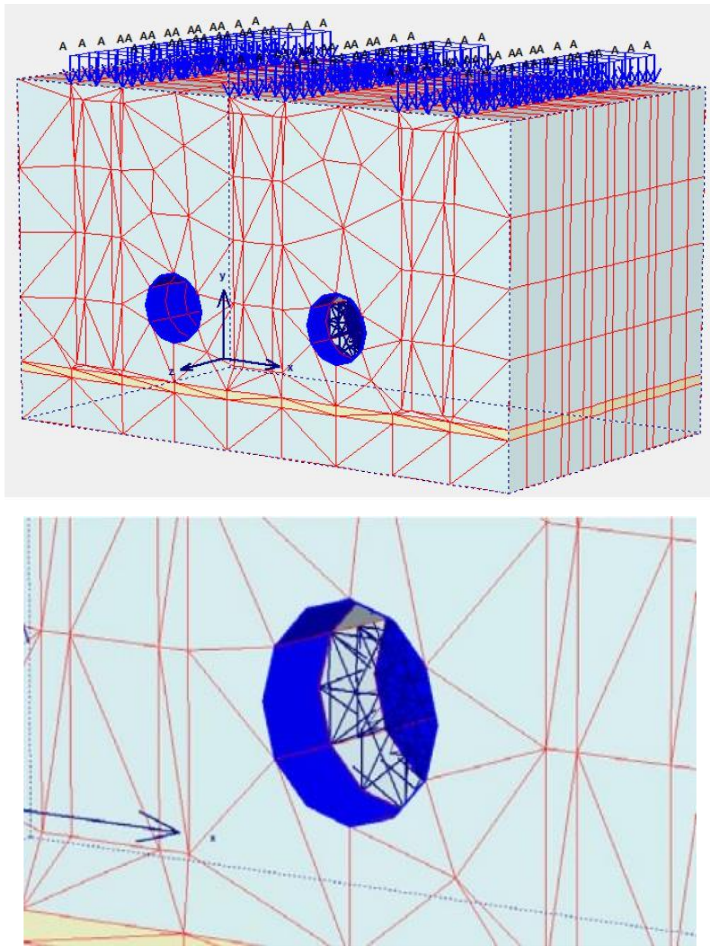

Figure 12
A complete drilling cycle with applied frontal and grout injection pressures and tunnel lining system

7 Modeling Results

According to the modeling performed, the results of the 14 and 18 m tunnel overburden in the ground and slab displacements are close together. Figures (13) and (14) show the displacement and impact results at two depths of 18 and 14 m.

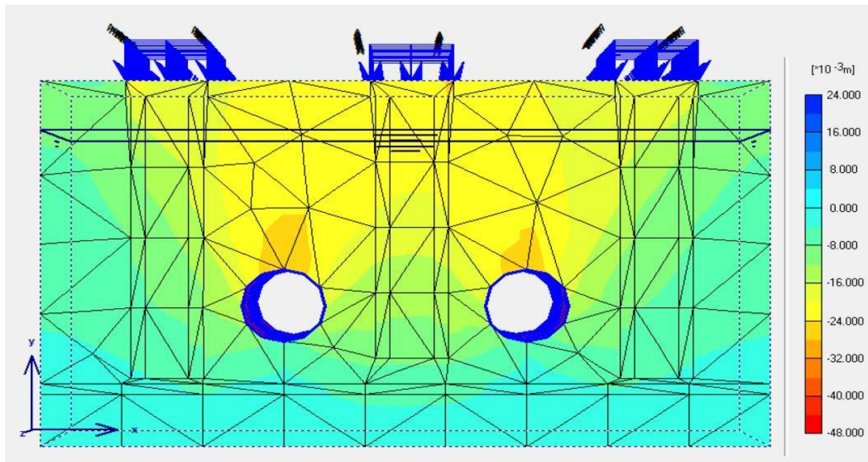

Figure 13
Displacement results and 18 m overburden impact area

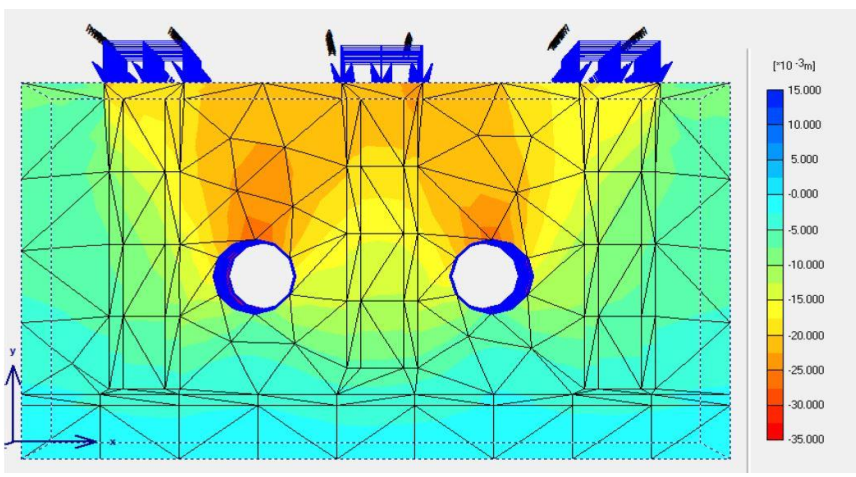

Figure 14
Displacement results and 14-meter overburden impact area

In order to study more precisely and compare the displacement of different points in two 14 mm and 18 m slopes, define the points in geometry and calculate all displacements at these points and are presented in Table (3) for both slopes. The location of each point is also shown in Fig. 15.

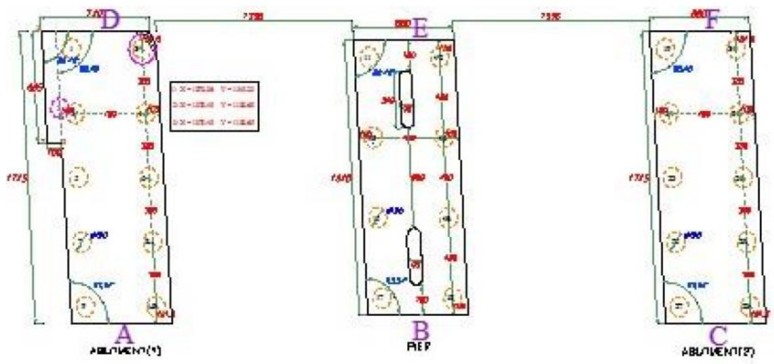

Figure 15
Specified points for tunnel displacement

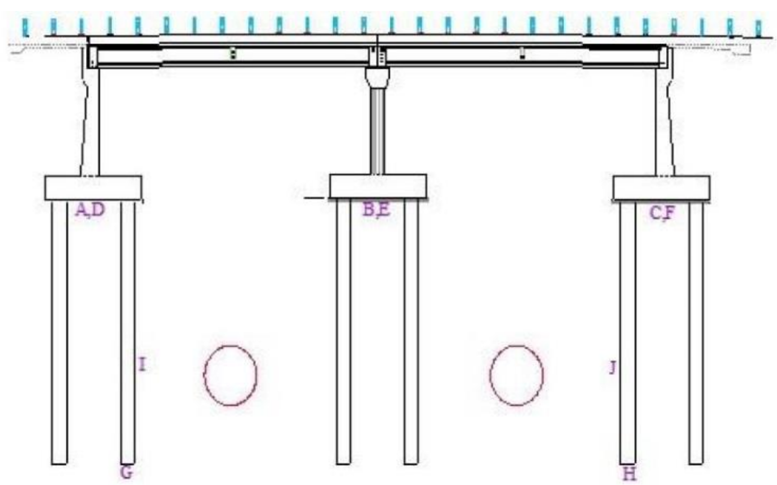

Figure 16
Specified points for tunnel displacement

Table 3
Displacement created at different points of the model in two overheads of 14 and 18 meters

Point	14 m Overburden	18 m Overburden
	Dis. (mm)	Dis. (mm)
A	17	17
B	20	22
C	14	15
D	13	13
E	15	16
F	11	12
G	11	12
H	11	12
I	15	15
J	13	14

As shown in the results of Table (3). The displacements caused by tunnel excavations at elevations of 14 and 18 m are not significantly different from each other, and these displacements are close to each other. Another important analytical parameter under consideration is over 18 m. Due to the 25 m depth of the pile slabs in the middle of the bridge, the tunnel floor to the pile tip is approximately 1.5 m in depth and this affects the capacity of the pile tip, which is one of the basic parameters of the pile at 18 m depth. Due to the depth of 14 meters, it is suggested that the design of the tunnel overpass under the 18 m overpass bridge be changed to 14 m over the 15 m overpass. Figure 16 illustrates the problem of tunnel impacts on the tip of the piles, which are 14 m deeper than 18 m deep.

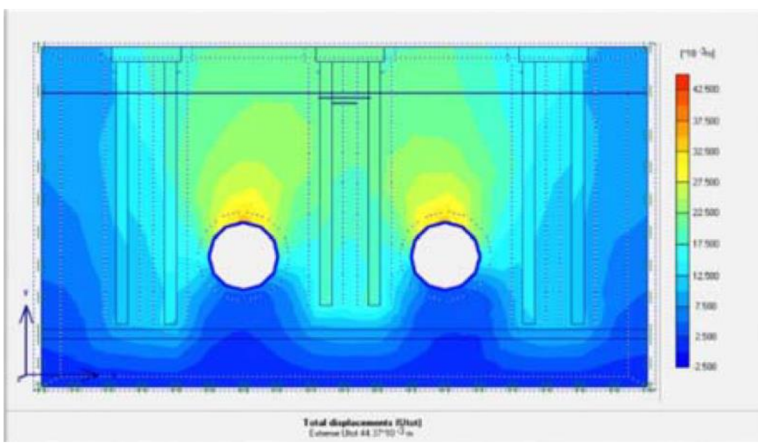

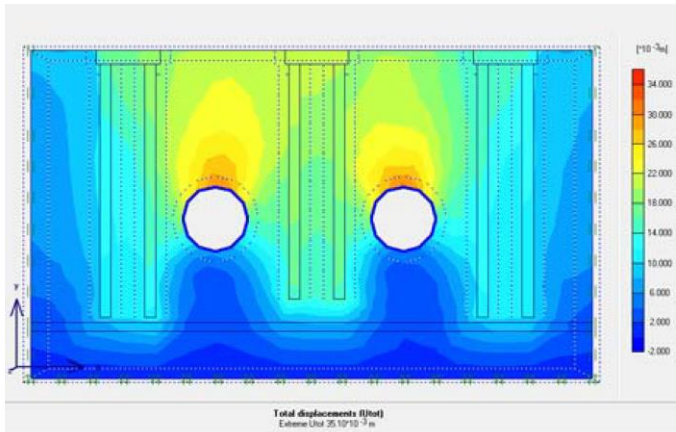

Figure 17
The total displacement area of the overpass tunnel 14 meters (Right) and 18 meters (Left) on the tip of the piles

Conclusions

The purpose of the authors of this study is to study, model and, if necessary, optimize part of the Shiraz 2 train route. The reason for choosing this section for consideration in this study is that the tunnel in this section passes under a non-planar inter-section (overpass bridge). At the beginning of the research, this route is introduced. Then the relevant basic concepts are presented and the calculations necessary to determine loads and load capacities are presented. The initial proposal for the tunnel depth consultant beneath the bridge was 18 meters. Due to the executive difficulties as well as the experiences of line 1, the authors suggested a depth survey of 14 meters. The modeling of the soil mass under the bridge was performed using the Plaxis software in two modes of 14 m and 18 m. Modeling has two important consequences: 1. The displacements caused by tunneling at depths of 14 and 18 meters were not different. 2. The slab piles are 25 meters deep in the middle of the bridge. In the 18-meter overburden, the tunnel floor is less distant to the tip of the pile and thus has a greater impact on the bearing capacity of the pile (compared to the 14 meters overburden). Therefore, the authors proposed to change the tunnel depth under the Mianrood Bridge, from 18 m to 14 m, according to the analysis.

References

1. Xu, W., P. Zhao, and L. Ning, *Last train delay management in urban rail transit network: Bi-objective MIP model and genetic algorithm.* KSCE Journal of Civil Engineering, 2018. 22(4): p. 1436-1445.

2. Chen, H., B. Jia, and S. Lau, *Sustainable urban form for Chinese compact cities: Challenges of a rapid urbanized economy.* Habitat international, 2008. 32(1): p. 28-40.

3. Mohammadzadeh, D., et al. *Urban train soil-structure interaction modeling and analysis*. in *International Conference on Global Research and Education*. 2019. Springer.

4. Mayer, T. and C. Trevien, *The impact of urban public transportation evidence from the Paris region.* Journal of Urban Economics, 2017. 102: p. 1-21.

5. Ding, R., et al., *Heuristic urban transportation network design method, a multilayer coevolution approach.* Physica A: Statistical Mechanics and its Applications, 2017. 479: p. 71-83.

6. Li, L., et al., *Urban transit coordination using an artificial transportation system.* IEEE Transactions on Intelligent Transportation Systems, 2010. 12(2): p. 374-383.

7. Knox, P.L. and L. McCarthy, *Urbanization: an introduction to urban geography*. 1994: Prentice-Hall Englewood Cliffs, NJ.

8. Tayyaran, M.R. and A.M. Khan, *The effects of telecommuting and intelligent transportation systems on urban development.* Journal of Urban Technology, 2003. 10(2): p. 87-100.

9. Saadin, H.K.a.M., *Analysis and Prediction of Land Surface Settlement Due to Tunneling (Case Study: Tabriz Urban Train Line 2 Project).* Transportation Engineering, 2010. 4.

10. Ng, C.W., H. Huang, and G. Liu, *Geotechnical Aspects of Underground Construction in Soft Ground: Proceedings of the 6th International Symposium (IS-Shanghai 2008)*. 2008: CRC Press.

11. Jongpradist, P., et al., *Development of tunneling influence zones for adjacent pile foundations by numerical analyses.* Tunnelling and underground space technology, 2013. 34: p. 96-109.

12. Selemetas, D., J. Standing, and R. Mair. *The response of full-scale piles to tunnelling*. in *Geotechnical aspects of underground construction in soft ground. Proceedings of the 5th international conference of TC 28 of the ISSMGE, the Netherlands, 15-17 june 2005*. 2006.

13. Schroeder, F.C., *The influence of bored piles on existing tunnels.* 2003.

14. Das, B.M. and K. Sobhan, *Principles of geotechnical engineering*. 2013: Cengage learning.